

THE ROLE OF NEGATIVE LINKS IN BRAIN NETWORKS.

...

Fabrizio Parente, Alfredo Colosimo

SAIMLAL Dept. , Sapienza University of Rome, Rome, Italy
fabrizio.parente86@gmail.com _alfredo.colosimo@uniroma1.it

Keywords: Negative Links, Balance Theory, Brain Network, Brain Areas, Multi Agent Systems.

Abstract: This paper provides a contribution to understand anti- (or negative) correlations between brain regions in fMRI studies. We report about: 1) characterizing negative correlations under physiological conditions through a careful analysis of records from healthy people; 2) reproducing a (homeostatic) equilibrium between different brain areas by a Multi Agent System and a negative retroaction mechanism on a small network model.

1 INTRODUCTION

1.1 Characterizing negative correlations.

A large fraction of studies on functional brain networks focused more on positive than on negative correlations between cerebral areas, due to the still not well defined nature of negative correlations. More recently, however, a growing attention in fMRI studies of the resting brain was dedicated to the anti- (or negative) correlation between brain regions. The early contributions dedicated to this phenomenon showed an anti-correlation between DMN and regions of the executive functions network (Greicius et al., 2003)(Uddin et al., 2009), attentional network (Fox et al., 2005), sensorial regions (Tian et al., 2007), as well as other areas of temporal, parietal and medial frontal regions (Uddin et al., 2009). A possible artifactual insertion of negative correlations in the analysis has been attributed to a preprocessing method called Global Signal Regression (GSR) which shifts the distribution curve of the correlations between the brain voxels to the right, and increases the proportion of negative values (Murphy et al., 2009).

Following a different approach to the fMRI signal correction, such as the intrascan *physiological parameters control* or the *white matter/cephalorachidian liquid* signal regression, several authors pointed out the persistence of significant negative correlations and a possible physiological role for them (Chai et al., 2012)(Chang and Glover, 2009)(Fox et al., 2009). In the absence of appropriate images correction methods such as the CompCor method (Behzadi et al., 2007), able to reveal negative correlations without increasing the proportion of spurious connections (Chai et al., 2012), it has been suggested that cardiac and respiratory processes can obscure the competitive dynamics between regions. By such methods the first principal components of the signal are regressed out from the white matter and cephalorachidian liquid, since signals from these regions seemed prone to correlate with heart and respiratory rate.

The main aim of this contribution is to characterize the negative functional connectivity at both single connection and whole network levels in the hope to clarify the biological properties of anti-correlations in human brain networks.

1.2 Modeling negative correlations.

A possible topology of negative functional networks has been described by a number of recent papers, in particular by means of the Network Theory (see below): Schwarz et al. (Schwarz and McGonigle, 2011) showed a probably random topology of networks only made by negative connectivity, while Chen et al. (Chen et al., 2011) found a relationship between the phase delay of positively connected node and the magnitude of negative correlations. In addition, Gopinath et al. (Gopinath et al., 2015) found that the hubs of the brain negative networks show several regulatory features, indicating a possible role in reciprocal modulation among sensorimotor cortex, limbic system and subcortical regions.

While the Network Theory is particularly useful in providing general quantifiers of network topology, the Balance Theory (see below) helps in defining the conditions for the networks' functional stability (Heider, 1946). This is of interest to us, since it may suggest possible mechanisms accounting for the influence of negative correlations on the functional equilibria between brain areas.

In this contribution we show how a simple 9-node network representing a crude model of 9 interacting brain regions, and implemented in a Multi Agents System, can account for the arrangement of both positive and negative correlations as well as for the homeostatic regulation between regions through a negative feedback mechanism.

2 MATERIALS AND METHODS.

2.1 Subjects.

The sample is composed by acquisitions of 180 healthy controls from the Beijing Zang dataset in the 1000 Functional Connectomes Classic collection (<http://fcon1000.projects.nitrc.org/indi/retro/BeijingEnhanced.html>). Resting data were obtained using a 3.0 T Siemens scanner at the Imaging Center for Brain Research, Beijing Normal University. A total of 240 volumes of EPI images were obtained axially (repetition time, 2000 ms; echo time, 30 ms; slices, 33; thickness, 3 mm; gap, 0.6 mm; field of view, 200x200 mm²; resolution, 64x64; flip angle, 90°). For the anatomical images a T1-weighted sagittal three-dimensional magnetization prepared rapid gradient echo (MPRAGE) sequence was acquired, covering the entire brain: 128 slices, TR= 2530ms, TE= 3.39ms, slice thickness= 1.33mm, flip angle= 7°, inversion time= 1100ms, FOV= 256x256mm, and in-plane resolution= 256x192.

Functional images were oriented to the twentieth scan, realigned and co-registered to the T1 image. Then the anatomical and functional images were normalized to standard space (EPI image in Montreal Neurological Institute coordinates) using the normalization parameters of the T1 image. Afterwards, a spatial gaussian filter was used (4x4x4mm), the motion parameters were regressed out and a band-pass filtering in the range 0.008-0.09 Hz was performed. Finally, in order to improve the characterization of negative functional connectivity, the anatomical CompCorr method (Behzadi et. al, 2007) was used to correct the images. SPM8 (Statistical Parametric Mapping, Wellcome Department of Cognitive Neurology, London, UK) and Functional Connectivity Toolbox (CONN), on MATLAB R2010b platform were used to perform the preprocessing.

2.2 Data preprocessing

The images of each subject were divided into 90 ROIs by the automatic anatomical labeling (Tzourio-Mazoyer et al., 2002) and from each ROI the time series of 240*2000 msec, namely 8 minutes, were extracted ¹. The correlation matrix was calculated for all possible couples of the 90 ROIs in each subject and this information was used in the form of a functional connectivity matrix (Friston, 2011). To choose a threshold for both negative and positive correlations, the False Discovery Rate (FDR; see Appendix 3) method (Glickman et al., 2014) was used and correlations with a significant p-value corrected for multiple comparisons (p-corrected < 0.05) were selected. Due to an incomplete connectivity in the negative network of some subjects, the threshold was exceeded in order to have a connected network. Hence, a new threshold for the FDR corrected p-value was set choosing the next higher p-value of correlations (for both negative and positive values). The matrix was then binarized and the

¹Notice that the volumes (240) correspond to the number of discrete points subjected to the statistical analysis.

Characteristic Path Length (CPL) calculated. The whole procedure was repeated until the CPL value became different from infinity, as expected in a connected network.

Forty-three subjects exceeded the p-values corresponding to the outliers in box-plot and were excluded from the analysis. Thus, a new threshold was set to 0.034, corresponding to $r = 0.14$, corrected to 0.064 by FDR, and the resulting matrix of each subject was splitted into two matrices only including positive or negative values, to be eventually binarized. Upon using the above threshold, the average Hamming distance between all the possible couples of matrices, to be taken as a similarity indicator, was 0.50 ± 0.03 .

2.3 Network functional indexes.

In fMRI studies the links are defined in terms of functional connectivity between nodes corresponding to ROIs localized in specific voxels (Bullmore and Bassett, 2011). From an Adjacency Matrix, AM, (see Appendix 1 for definitions and details) the following indices were calculated in both positive and negative networks: network density (or cost), clustering coefficient (CC), Characteristic Path Length (CPL), gamma (γ), lambda (λ), sigma (σ), local and global efficiency, assortativity and Node Degree (k).

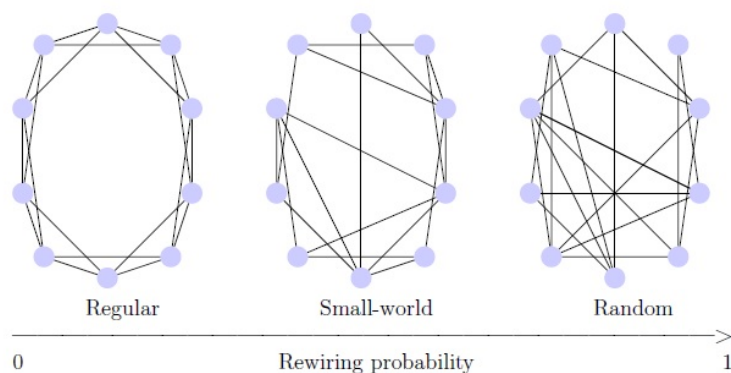


Figure 1: *Smallworld model*. Intermediate location of Smallworldness in the Regular-to-Random transition of a network as a function of links rewiring. The rewiring probability is the probability of any edge in the Regular state to be rewired into the graph as a random edge (Watts and Strogatz, 1998).

By consideration of the above indexes, several network types can be distinguished as regular network (or lattice-like), random network, scale-free and small-world network. Figure 1 shows the last one, which is widely used to characterise a link pattern intermediate between a fully ordered and a completely random condition.

In order to study the node degree distribution the following statistical distributions were used: Power law, Exponential, Poisson and Truncated Power Law (Achard et al., 2008). In each case the mean squared error (MSE) between the cumulative distribution of empirical data and the theoretical cumulative distribution was calculated. A two-way ANOVA was used to check any difference in MSE values: as for the statistical distribution factor with 4 levels (Power Law, Exponential, Poisson and Truncated Power Law), as for the sign factor with 2 levels (positive and negative network).

To describe specific topological features of networks a number of *ad hoc* indexes have been used, such as the global and local *Efficiency* (Latora and Marchiori, 2001), and the correlation degree or *Assortativity* (Newman, 2002). The latter metric calculates the probability of interaction among nodes: in the case of positive correlations, nodes tend to connect between each other on the basis of similar node degree, and the network is called *assortative*. Conversely, in the case of negative correlations nodes tend to be connected to nodes with different node degree, and the network is called *disassortative*. A related index is the *Rich-Club* coefficient (van den Heuvel and Sporns, 2011), which indicates a particular range of node degree where the probability of finding nodes connected to nodes with the same node degree is higher than the corresponding random value. Networks having a high Rich-Club coefficient show the *Rich-Club effect*, meaning that the "rich" nodes tend to connect among each other but not with lower degree nodes. Since the opposite situation is also possible, when a lower Rich-Club coefficient refers to a structure where highly connected nodes tend to avoid reciprocal links, we defined *repulsion interval* such node degree range. Hence, in the aim to establish the presence of nodes with a repulsion between each other, a Rich-Club method (van den Heuvel and Sporns, 2011) was used: the Rich-Club coefficient of the original network, the corresponding random value and their ratio, namely a normalized Rich-Club coefficient, were calculated². The random values of each degree (k) were calculated as the average of 100 randomization cycles. The rich-club coefficient of real networks and random networks were then compared by a Wilcoxon rank sum test for each degree (k) and Bonferroni corrected for multiple comparisons.

²A rich-club interval is defined as the range of nodes with a given node degree in which the rich-club coefficient is higher than the corresponding random, as well as the normalized rich-club coefficient is greater than 1. Conversely, a repulsion interval is defined as the node degree range in which the rich-club coefficient is lower than the corresponding random.

Finally, the *Centrality* of nodes was studied using the node degree of each cerebral region and central regions evaluated by a box-plot analysis. All calculations were carried out by means of the Brain Connectivity Toolbox (Rubinov and Sporns, 2009) and an original script in Matlab.

2.4 The Balance Theory.

The concept of *balance* was proposed by Heider in 1946 (Heider, 1946) and refers to a triadic *pox* model in which an agent *p* has a positive or negative relation to another agent *o*, and both have a positive or negative relation to a third agent *x*. The triangular graph is balanced (or stable) if cycling through it (by multiplying the links) produces a positive result. In order to get that, the links must be all positive or two negative and one positive. In an unbalanced (or unstable) triangle the links are all negative or two positive and one negative, in agreement with the algebraic rule of sign multiplication. Cartwright and Harary extended this logic from a triadic relation to a network with more than three agents and their result is summarized by the *First Structure Theorem* : if a graph is balanced the nodes can be partitioned into two subsets such that ties between nodes within a subset are all positive, and ties between nodes in different subsets are all negative (Cartwright and Harary, 1956).

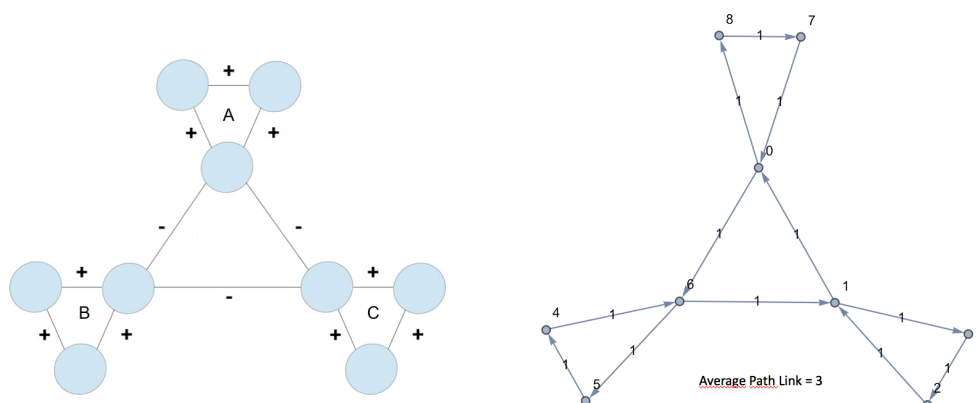


Figure 2: Example of a stable network including modules and links of specific sign or direction. Stability is obtained by **Left** : the opposite sign of links within and between, respectively, the A, B, and C modules; **Right** : the clockwise and anticlockwise direction of links within and between modules. The nodes are indicated by numbers (0 ... 8) and the links by weights which, in the case of binary networks, = 1. See the text for details and Appendix 1 for the Adjacency Matrix of the model on the right.

Davis proposed a generalization of this theorem considering the all-negative triangle as balanced and hence a signed network as balanced if it contains no cycle with a single negative edge (Davis, 1967). From this reformulation it is possible to define the *Second Structure Theorem*: the nodes can be divided in more than two subclusters containing only positive ties, while negative links are permitted among nodes belonging to different clusters. For more information (Norman and Doreian, 2003) (Doreian and Mvar, 2009).

In Figure 2 is reported (left side), the scheme of a 9-node graph including three stable modules (A,B,C) connected among each other by negative connections. In agreement with the *Second Structure Theorem* this global link pattern corresponds to stability. On the right side of the figure the drawing obtained by an original Mathematica™ routine is reported, where the same architecture is drawn in terms of *directed* links from a "source" node to a "target" node. The stability in the scheme on the left can be reproduced, as testified by the finite value (= 2) of the <ShortestPathLength> (APL) if and only if the clockwise\anticlockwise direction of each links on the right model corresponds to the positive\negative sign of the corresponding link on the left. Worthless to say that also the specular correspondence between sign and direction holds.

2.5 MAS-based Simulation of networks' dynamics.

MAS (Multi Agent Systems) based simulations provide an almost ideal tool to mimate phenomena involving a population of "agents" interacting among each other and with the environment (Wilenski, 1999). Their most appealing features emerge in the study of dynamical phenomena and make them of great utility in the set-up of time dependent mechanistic models. (Colosimo, 2008).

Figure 3 shows the same 9-node network architecture based upon directional links as in Figure 2 (right panel) now reproduced in the NetLogo™ MAS programming environment (<https://ccl.northwestern.edu/netlogo/>). Thanks to the dynamic features of the environment, the activation signal traveling from an input node to an output node is easily reproduced and can be visualized in terms of time dependent changes in the apparent size of nodes.

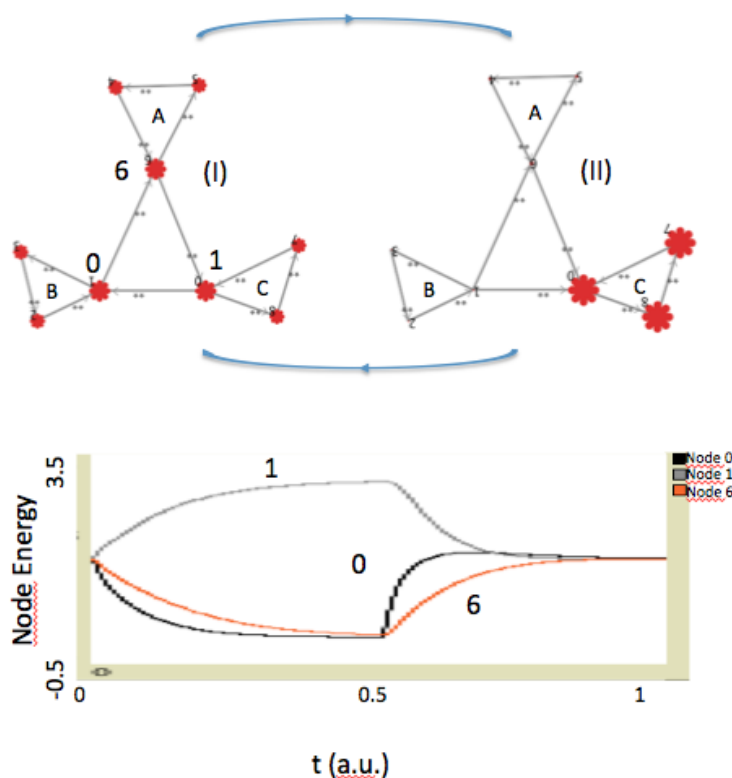


Figure 3: *Dynamic features of the 9-node network in Figure 2, right panel. The direction of the link between nodes 0, 1 is 0 → 1 in (II) and 1 → 0 in (I). The latter is the only one compatible with a global stability. The (I) → (II) and (II) → (I) transitions start at t = 0 and t = 0.5, respectively. The bottom graph describes the consequential time-dependent changes in activity (size) of nodes 0, 1 and 6 (representative of the three subnetworks) See the text for details.*

Notice that at t = 0 the initial energy level = 1 of all nodes in the network corresponds to the (I) state; this "balanced" energy condition, after a strong unbalance due to the (I) → (II) transition, is only restored when the opposite transition occurs at t = 0.5. Figure 3 exemplifies the type of dynamic detail which can be obtained by a minimum programming effort setting up a MAS network model in the NetLogo environment.

3 RESULTS

3.1 Node degree distributions and general indicators of functional negative networks.

Table 1 contains mean indexes values calculated on positive and negative networks. The negative networks are characterized by a lower density and lower average node degree values as compared to positive networks. The clustering coefficient and the local efficiency of negative networks describe a low segregated structure, while the CPL and the global efficiency are similar for both networks. These last indices show clearly that negative networks are not well described by the small-world model (also recognized by the low values of γ and σ), while the negative value of assortativity can be assumed as an indication for an alternative non-random structure of these networks.

To test the possible non-random nature of negative networks, we will compare the degree distribution of brain negative networks using a Poisson distribution and others distributions relevant for the characterization of the network topology. As for the characterization of the degree distribution, the ANOVA analysis showed a significant effect of the distribution factor ($p < 0.0001$, $F=13.88$, $df=3$). In particular, post-hoc analysis (see Figure 4) pointed out that the MSE of the truncated power law distribution was significantly lower than for other distributions (Bonferroni corrected p-values > 0.0001). No significant effect of the sign factor was found ($p=0.087$, $F=3.01$, $df=1$). In table 2 are summarized the mean parameters of the truncated power law distribution.

Finally, central nodes of negative networks were found in the right inferior parietal lobule (no supramarginal and angular gyri, 28.7 ± 10.5), right middle frontal gyrus (28.6 ± 10.1), left middle frontal gyrus (26.9 ± 9.9) and right inferior frontal gyrus, opercular part (26.7 ± 9.6), see the left box-plot in Figure 5.

	Negative network mean (sd)	Positive network mean (sd)
Network density	0.22 (0.03)	0.46 (0.03)
Clustering Coefficient	0.07 (0.02)	0.61 (0.04)
Characteristic Path Length	1.93 (0.11)	1.64 (0.05)
γ	0.23 (0.07)	1.40 (0.12)
λ	1.19 (0.09)	1.02 (0.01)
σ	0.20 (0.07)	1.38 (0.11)
Global Efficiency	0.58 (0.03)	0.69 (0.02)
Local Efficiency	0.14 (0.06)	0.80 (0.02)
k	17.63 (3.10)	34.26 (3.52)
Assortativity	-0.36 (0.10)	0.26 (0.09)

Table 1: Indices of positive and negative networks.

	k_c mean (sd)	α mean (sd)
Positive network	18.78 (13.66)	3.34 (0.81)
Negative network	8.31 (3.39)	2.82 (0.82)

Table 2: Values of k^c and α , parameters of the truncated-power law model.

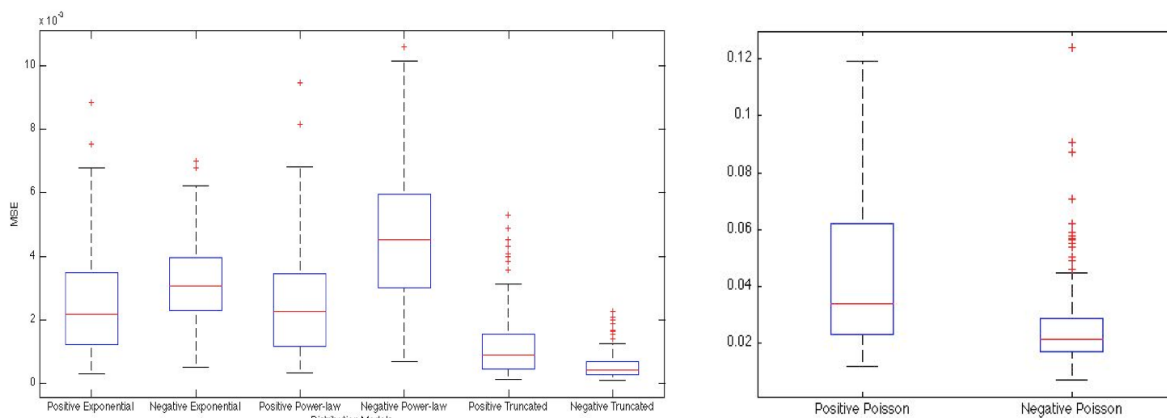


Figure 4: Box-plot of the mean square error (MSE). Labeling of distribution models (from left to right): Positive Exponential, Negative Exponential, Positive Power-law, Negative Power-law, Positive Truncated Power-law, Negative Truncated Power-law, Positive Poisson, Negative Poisson. See the text for details.

3.2 Rich-Club analysis.

As a consequence of the low connection probability between two nodes with the same node degree, a repulsion between nodes with given node degree is possible³, then we study the Rich-Club organization of negative networks. The analysis showed that shared edges between nodes decrease as a function of the increasing node degree (Figure 6). From the statistical analysis, a clear difference from random networks was reached at the highest values of node degree (node degree > 13, p-value < 0.05 Bonferroni corrected). Hereafter, we call this range "repulsion interval".

3.3 Modeling subnetworks equilibria through a negative feedback by a MAS.

An appealing feature of MAS, emphasized by the friendly NetLogo environment, is the straightforward rearrangement of links according to even sophisticated rules. In the case at hand, such rules smooth the difference in the activity levels among

³This phenomenon would be the opposite of the Rich-Club organization already found in brain positive networks and we explored the use of the Rich-Club coefficient in order to clarify this network property.

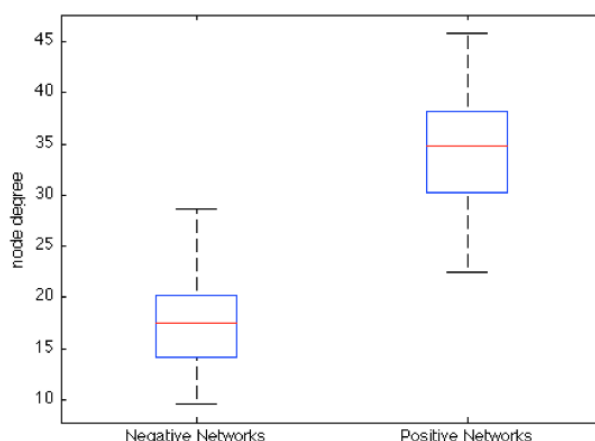


Figure 5: *Box-plot of node degree centrality*. Left plot negative networks; right plot positive networks (central nodes positive networks: bilateral superior temporal gyrus (temporal pole), right parahippocampal gyrus, right superior temporal gyrus).

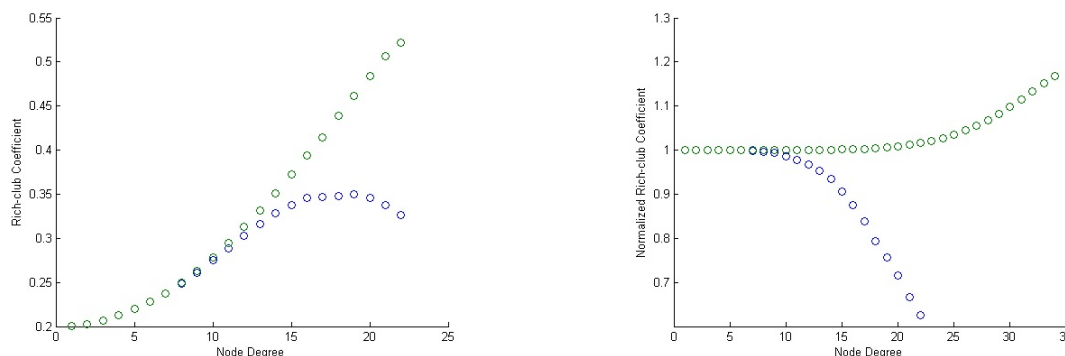


Figure 6: *Rich-Club coefficient and normalized Rich-Club as a function of Node Degree*. Upper panel Rich-Club coefficient: blue dots original network, green dots random network; bottom panel normalized Rich-Club coefficient: blue dots negative networks, green dots positive networks. The Rich-Club phenomenon the positive networks is reached for Node Degree higher than 26 (p-value bonferroni corrected < 0.05).

subnetworks by reversing the sign of some links or even forming new links of reversed sign, the final aim being a more stable condition of the whole network. As shown in Figure 7, an intuitive dynamical representation of the network global activation states can be obtained making the nodes' size proportional to the activation level which, in turn, depends upon the energy (information) flowing through the links (see also Figure 3). Thus, in order to overcome the unbalanced state (0), a new link of appropriate sign can in principle be formed involving one of three different couples of nodes, as shown in (I), (II) and (III). Only in last case the global pattern of signs, as defined in the table on the bottom left of the figure, guarantees a global stability state, in agreement with the "Second Stability Theorem" (see Methods). Notice that:

- in the (I) and (II) conditions, the global instability produces a oscillatory regime of activation, as shown by the time courses in the middle panels of the figure;
- the oscillations in the time courses reflect the autonomous generation in the network of an extra link whenever (as in the 0 state) a given threshold in the energy of some node is trespassed;
- the new link generated in (I) and (II), however, can only relieve the system from the surplus of energy in the a subnetwork; they cannot guarantee the stability of an equilibrium state (S). Soon after brushing such an equilibrium (S), a new cycle is immediately initiated.
- Solely in state (III) the global link pattern is in favor of a stable equilibrium.

Thus, the role of restoring a global stability in the network is assigned to the emergence of a new subnetwork in a specific location with a specific link architecture (see the (III) pattern in Figure 7). It is quite interesting to notice that the above

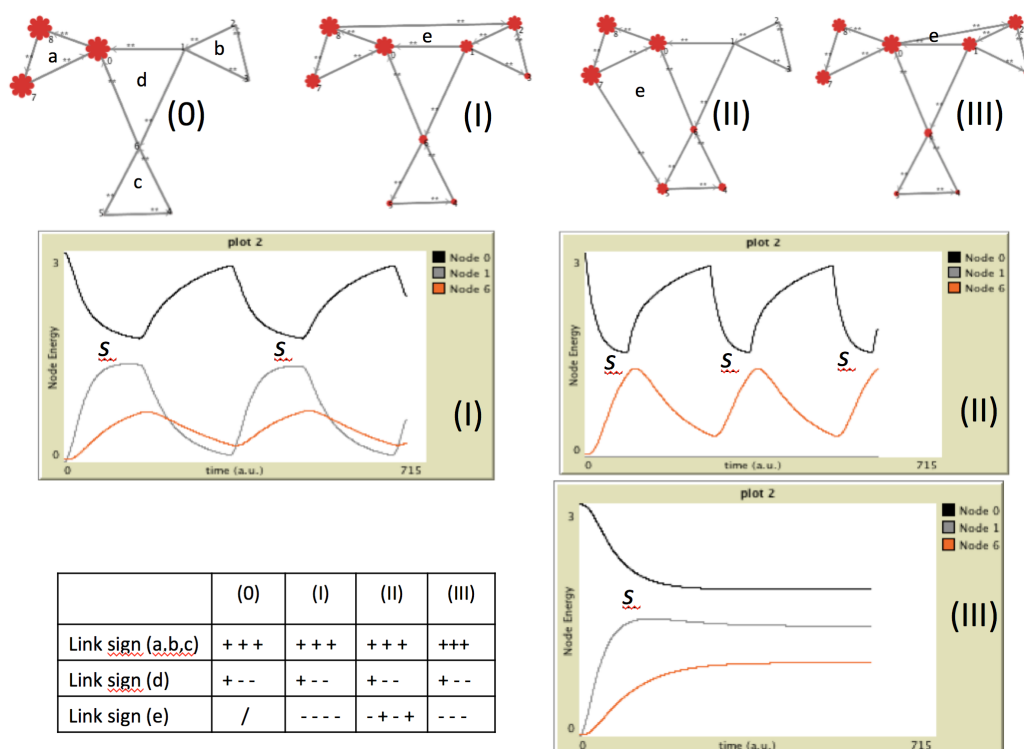


Figure 7: *Simulating homeostatic equilibria of subnetworks by MAS.* The architecture of the network is the same as in Figure 3. From an initial state characterized by the hyperactivity of the a subnetwork in (0), a more balanced global configuration can be reached by activating some extra link between the nodes in a and nodes in subnetworks b and c. This gives rise to a new subnetwork e, located in different possible locations, three of which are represented in (I), (II), and (III). The table in the lower left corner contains the sign of the links in the subnetworks of the more balanced (III), less balanced (0) and intermediate (I, II), networks. The "S" indicate the energy level corresponding to an equilibrium state.

mechanistic picture is strongly reminding the "negative feedback" mechanism so often invoked to describe the modulation of physiological equilibria in metabolic cycles. However, at odds with metabolic cycles, where the chemical nature (or concentration) of substance(s) flowing through the direct and inverse pathways are different, in the present case the activation level of the target node is the essential trigger of the negative feedback.

4 DISCUSSION

4.1 Topological properties of negative networks.

Negative functional networks appear quite different from random networks. In a such a context a crucial issue concerns their possible artifactual nature since, for example, Murphy et al. (Murphy et al., 2009) found a clear artifactual insertion of negative correlations between BOLD signals of brain voxels due to GSR. In addition, some characteristics of a random topology in negative functional networks using GSR in the preprocessing step were also found by Schwarz (Schwarz and McGonigle, 2011). In order to filter the cardiac and respiratory noise out of the BOLD signal, we used the CompCorr method, which supposedly reduces the artifactual negative correlations (Behzadi et al., 2007). At odds with Schwarz et al., our results point to a non-random nature of negative functional networks, as indicated by a truncated power-law distribution and by a non-zero assortativity value. On the same networks we actually noticed a low Clustering Coefficient (CC), generally associated to random networks, which however could indicate, more than a random topology, a non-segregated organization.

In positive networks high CC values indicate an efficient segregation in the information transfer which, together with a low Characteristic Path Length (CPL) value, makes a small-world topology an optimal compromise between segregation and integration properties. On the other hand, in negative networks this could not be necessarily due to a different role of

anti-correlations in the whole brain. Thus, the low value of CC may be an indication that negative functional networks cannot be described by the classical model of small-world topology and a different model is required in that case.

To test an alternative model, we used a Rich-Club analysis to explore other features associated to the topology of negative functional networks and, in particular, the observed negative assortativity (or disassortativity). In fact, in positive networks the positive value of assortativity indicates the probability of nodes to get connected to nodes with the same node degree. The Rich-Club analysis, clarifies that this average trend of probability is kept only by the most connected nodes, corresponding to a *structural core* of highly connected brain regions (Crossley et al., 2016). In negative networks, exactly at odds with positive networks, the disassortative feature is caused by a repulsion between nodes of the same node degree and our Rich-Club analysis shows that this repulsion is only significant in central nodes, within a given node degree window *the repulsion interval*.

The architecture emerging from our analysis describes the presence of a relatively small number of central nodes less connected between each other but interacting with nodes of lower degree. This indicates: 1) a possible organization in which central nodes can modulate other regions without interfering with other central nodes, and 2) a possible sharing of information only at the lower level of node degree. An open question concerns how negative interactions are related to healthy (or pathological) brain activity and how to include both positive and negative interactions in a unique and comprehensive frame.

At present, a modelistic approach to the above questions appears most useful not only for the general ability of abstract models to propose an acceptable rationale even for intricate, empirical findings, but also, particularly in the case of very complex systems like those at hand, to anticipate some of their unexpected, features.

4.2 Network stability and sign of ties.

Using a MAS based simulation engine to study the functional properties of a neuronal network is simplified by the straightforward identification of MAS agents and links with, respectively, network nodes and ties. In a MAS representation of a neuronal network, in fact, an agent can be assimilated to a single neuron, to a set of functionally correlated neurons or even to a given brain region so that functional relationships among subnetworks, are not necessarily associated to well defined anatomical connections. In such an abstract perspective if, on one hand, one must face the scarcity of detailed and precise experimental information, on the other hand he/she can take advantage of a considerable number of degrees of freedom in the set-up of models. Obvious as it is, the necessary prerequisite of the modelistic results, as for any model of any system, must include strict self-consistency and solid realism.

At our knowledge, the simulations of functional regulation phenomena presented here in a simple network are almost unique in the use of a bottom-up approach, where the local interactions between couples of nodes (neurons) induce the emergence of a global behavior of the neuronal population pointing to an homeostatic equilibrium. A direct comparison with an analytical strategy of dynamical simulations based on differential equations would probably be not in favor of our approach in terms of speed and efficiency. However, the conclusion would more probably be just the opposite after taking into account the great advantage of a close, intuitive correspondence between in vivo and in silico events.

Finally, the relatively tiny size and specific architecture of the 9 node network used here has been purposely designed to include both positive and negative connections among functional modules (subnetworks). It is worth noticing that such a minimalistic structure, coupled to the underlying MAS programming environment, showed able to reproduce some relatively sophisticated homeostatic phenomena (see Figure 7) and its possible extension to the study of stability alterations of pathological significance is in due course.

ACKNOWLEDGEMENTS

We want to thank sincerely in particular one anonymous referee for a number of suggestions useful to improve the quality of our contribution.

REFERENCES

- Achard, S., Salvador, R., Whitcher, B., Suckling, J., and Bullmore, E. (2008). A resilient, low-frequency, small-world human brain functional network with highly connected association cortical hubs. *J. Neurosci.*, 26(1):63–72.
- Behzadi, Y., Restom, K., Liau, J., and Liu, T. (2007). A component based noised correction method (compcor) for bold and perfusion based fmri. *Neuroimage*, 37(1):90–101.
- Bullmore, E. and Bassett, S. (2011). Brain graphs: Graphical models of the human brain connectome. *Annu. Rev. Clin. Psychol.*, 7.
- Cartwright, D. and Harary, F. (1956). Structural balance: a generalization of heider's theory. *Psychological Review*, 63:277–293.

- Chai, X., Castanon, A., Ongur, D., and Whitfield-Gabrieli, S. (2012). Anticorrelations in resting state networks without global signal regression. *Neuroimage*, 59(2):1420–8.
- Chang, C. and Glover, G. (2009). Effects of model-based physiological noise correction on default mode network anti-correlations and correlations. *Neuroimage*, 44(4):1448–59.
- Chen, G., Chen, G., Xie, C., and Li, S. (2011). Negative functional connectivity and its dependence on the shortest path length of positive network in the resting-state human brain. *Brain Connect.*, 1(3):195–206.
- Colosimo, A. (2008). Biological simulations by autonomous agents: two examples using the netlogo environment. *Biophysics and Bioengineering Letters*, 1(3):40 – 50.
- Crossley, N., Fox, P., and Bullmore., E. (2016). Meta-connectomics: human brain network and connectivity meta-analyses. *Psychol Med.*, 46(5):897–907.
- Davis, J. (1967). Clustering and structural balance in graph. *Human Relation*, 20:181–187.
- Doreian, P. and Mvar, A. (2009). Partitioning signed social networks. *Social Networks*, 31:1–11.
- Fox, M., Snyder, A., Vincent, J., Corbetta, M., Essen, D. V., and Raichle, M. (2005). The human brain is intrinsically organized into dynamic, anticorrelated functional networks. *Proc Natl Acad Sci USA*, 102:9673–9678.
- Fox, M., Zhang, D., Snyder, A., and Raichle, M. (2009). The global signal and observed anticorrelated resting state brain networks. *J Neurophysiol.*, 101(6):3270–328.
- Friston, K. (2011). "functional and effective connectivity: a review. *Brain Connectivity.*, 1(1):13–36.
- Glickman, M., Rao, S., and Schultz, M. (2014). False discovery rate control is a recommended alternative to bonferroni-type adjustments in health studies. *J Clin. Epidemiol.*, 67(8):850–857.
- Gopinath, K., Krishnamurthy, V., Cabanban, R., and Crosson, B. (2015). Hubs of anticorrelation in high-resolution resting-state functional connectivity network architecture. *Brain Connect.*, (4):308–315.
- Greicius, M., Krasnow, B., Reiss, A., and Menon, V. (2003). Functional connectivity in the resting brain: a network analysis of the default mode hypothesis. *Proc Natl Acad Sci U S A*, 100:2531–2258.
- Heider, F. (1946). Attitudes and cognitive organization. *Journal of Psychology*, 21(17):107–112.
- Latora, V. and Marchiori, M. (2001). Efficient behavior of small-world networks. *Phys Rev Lett.*, 87(19).
- Murphy, R., Birn, R., Handwerker, D., Jones, T., and Bandettini, P. (2009). The impact of global signal regression on resting state correlations: Are anti-correlated networks introduced? *Neuroimage*, 44(1):893–905.
- Newman, M. (2002). Assortative mixing in networks. *Phys. Rev. Lett.*, 89:208701.
- Newman, M. (2006). Modularity and community structure in networks. *Proc. Natl. Acad. Sci. U. S. A.*, 103:8577–8582.
- Norman, N. and Doreian, P. (2003). Some dynamic of social balance processes: Bringing heider back into balance theory. *Social Network*, 25:17–49.
- Rubinov, M. and Sporns, O. (2009). Complex network measures of brain connectivity: uses and interpretations. *Neuroimage*, 53(3):1059–69.
- Schwarz, A. and McGonigle, J. (2011). Negative edges and soft thresholding in complex network analysis of resting state functional connectivity data. *Neuroimage*, 55(3):1132–46.
- Tian, L., Jiang, T., Liu, Y., Yu, C., Wang, K., Zhou, Y., Song, M., and Li, K. (2007). The relationship within and between the extrinsic and intrinsic systems indicated by resting state correlational patterns of sensory cortices. *Neuroimage*, 36(3):684–90.
- Tzourio-Mazoyer, N., Landeau, B., Papathanassiou, D., Crivello, F., Etard, O., Delcroix, N., Mazoyer, B., and Joliot, M. (2002). Automated anatomical labeling of activations in spm using a macroscopic anatomical parcellation of the mni mri single-subject brain. *NeuroImage*, 15(1):273–289.
- Uddin, L., Kelly, A., Biswal, B., Castellanos, F. X., and Milham, M. (2009). Functional connectivity of default mode network components: correlation, anticorrelation, and causality. *Hum. Brain Mapp.*, 30:625–637.
- van den Heuvel, M. and Sporns, O. (2011). Rich-club organization of the human connectome. *J Neurosci.*, 31(44).
- Watts, D. and Strogatz, S. (1998). Collective dynamics of 'small-world' networks. *Nature*, 393:440–442.
- Wilenski, U. (1999). <http://ccl.northwestern.edu/netlogo/>.

APPENDIX 1

The Adjacency Matrix

According to the *Network Theory*, a network is defined as an ensemble of N nodes linked by K edges. Three different types of networks may be distinguished, whether links are directed, weighted, or in binary form. In all cases, the link structure may be arranged in an $N \times N$ square matrix, named Adjacency Matrix (AM), where the i, j location indicates the absence/presence of a link between the i and j nodes (for binary networks) or its weight (for non binary networks). The scheme below reports the binary AM representing the undirected version of the network in figure 2 (right). The directed version corresponds to the upper (or lower) diagonal half matrix.

```
[ 0 1 0 0 0 0 1 1 1 ]
[ 1 0 1 1 0 0 1 0 0 ]
[ 0 1 0 1 0 0 0 0 0 ]
[ 0 1 1 0 0 0 0 0 0 ]
[ 0 0 0 0 0 1 1 0 0 ]
[ 0 0 0 0 1 0 1 0 0 ]
[ 1 1 0 0 1 1 0 0 0 ]
[ 1 0 0 0 0 0 0 0 1 ]
[ 1 0 0 0 0 0 0 1 0 ]
```

APPENDIX 2

Generalities

In fMRI studies the links of a neuronal network represent functional connectivities between nodes corresponding to ROIs localized in specific voxels (Bullmore and Bassett, 2011). Deriving a graph from the AM is straightforward, as well as deriving the following describing indexes.

- CC = *Clustering Coefficient* as an index of segregation;
- CPL = *Characteristic Path Length* as an index of integration;

By consideration of the above mentioned indexes, the following graph typologies can be distinguished:

- *regular* or *lattice-like* type: high CC and low CPL ;
- *random* type: high CPL and low CC ;
- *small-world* type: intermediate CC and CPL ; A *Small World* architecture allows to speed up the communication among distant nodes thanks to a relatively small number of shortcuts, thus making logarithmic the dependencies of the CPL on the network size N (Watts and Strogatz, 1998). In order to get a network with a small world topology, a rewiring procedure of edges with a given probability p is shown in (Figure 1): Starting from a regular network, in which each node is connected to its second nearest neighbors, a number of links are rewired to a randomly chosen node with a probability p
- *scale-free* type: low level of CPL and intermediate CC between *random* and *small-world* types (power law distribution of Node Degrees). This gives an inhomogeneous degree distribution characterized by the simultaneous presence of a few central nodes and a large number of poorly connected nodes.

In addition two other indexes have been proposed to characterize network topologies, namely: *global* and *local efficiencies* (Latora and Marchiori, 2001), appropriate for estimating the communication level between nodes in whole network as well as in their subnetworks; and the *modularity*, indicating the presence of subnetworks (Newman, 2006).

Notation

- N = total number of nodes in the network
- L = total number of links in the network
- (i, j) = is a link between i and j nodes
- a_{ij} = link value between nodes i and j (= 0/1 in binary networks)

<i>Name/abbreviation(Symbol)</i>	<i>Definition</i>
Node Degree / ND (k_i)	# of links of node i
Node Degree distribution	# of nodes with degree k ($k = 0, 1, 2, \dots$)
Clustering Coefficient / CC (C_l)	$C_l = \frac{2e_i}{k_i(k_i-1)}$ <p>k_i: # of neighbors of node i e_i: # of connected pairs within all neighbors of node i</p>
Shortest Path Length / SPL (L_{ij})	Minimum # of links between nodes i and j :
Characteristic Path Length / CPL	also Average Path Length (see below)
Network density	$0 \leq k = \frac{2*\epsilon_\tau}{N(N-1)} \leq 1$ <p>where ϵ_τ is the number of links associated to a given (τ) threshold.</p>
Global Efficiency	$E = \frac{1}{N} \sum_{i \in N} \frac{\sum_{j \in N, i \neq j} d_{ij}^{-1}}{N-1}$ <p>with $d_{jh}(N_i)$ is the length of the shortest path between j and h, that contains only neighbors of i.</p>
Local Efficiency	$E_{loc} = \frac{1}{N} \sum_{i \in N} \frac{\sum_{j, h \in N, j \neq i} a_{ij} a_{ih} [d_{jh}(N_i)]^{-1}}{k_i(k_i-1)}$ <p>with $d_{jh}(N_i)$ is the length of the shortest path between j and h, that contains only neighbors of i.</p>
Gamma / (γ)	CC of a network normalized to the corresponding random network $(\gamma > 1$ in the <i>small world</i> networks).
Lambda / (λ)	CPL of a network normalized to the corresponding random network (about 1 in the <i>small world</i> networks).
Small-Worldness / (σ)	$S > 1$ in <i>Small World</i> networks. $S = \frac{CC/CC_{rand}}{CPL/CPL_{rand}}$
Assortativity	$r = \frac{l^{-1} \sum_{(i,j) \in L} k_i k_j - [l^{-1} \sum_{(i,j) \in L} 1/2(k_i + k_j)]^2}{l^{-1} \sum_{(i,j) \in L} 1/2(k_i^2 + k_j^2) - [l^{-1} \sum_{(i,j) \in L} 1/2(k_i + k_j)]^2}$
Rich-club coefficient	$\phi(k) = \frac{2l_{\geq k}}{n_{\geq k}(n_{\geq k}-1)}$ with $n_{\geq k}$ <p>number of nodes that have greater or equal node degree than k, and $l_{\geq k}$ number of links between that $n_{\geq k}$ nodes.</p>
Normalized rich-club coefficient	$\Phi_{norm}(k) = \frac{\phi(k)}{\Phi_{random}(k)}$ <p>with $\Phi_{random}(k)$ the average rich-club coefficient of m random networks.</p>

Table 3: Name and definition of the network parameters used in this work.

APPENDIX 3

False Discovery Rate (FDR) method.

The original FDR method by Benjamini and Hochberg (Benjamini and Hochberg, 1995), can be schematized as follows:

- For n multiple tests choose the maximum false discovery rate d (0.05 in our case);
- Sort the n p-values of single test in ascending order and denote this probability p_i from p_1 (the lower probability) to p_n (the highest probability);
- Calculate the p_k for which $p_i \leq d \cdot i/n$ for all the i ;
- All tests with p-value lower than p_k are declared as significant.

The method has been implemented in a Matlab script and can be made available upon request to one of the authors (F.P.).